International Journal of Antimicrobial Agents 53 (2019) 500–507

Contents lists available at ScienceDirect

International Journal of Antimicrobial Agents

journal homepage: www.elsevier.com/locate/ijantimicag

Antimicrobial efficacy and mechanism of action of poly(amidoamine) (PAMAM) dendrimers against opportunistic pathogens

Amy M. Holmes[a,*], Jon R. Heylings[b], Ka-Wai Wan[a,†], Gary P. Moss[a,‡]

[a] School of Pharmacy, Keele University, Keele, Staffordshire ST5 5BG, UK
[b] Dermal Technology Laboratory Ltd., MedIC4, Keele University Science and Innovation Park, Keele, Staffordshire, ST5 5NL, UK

ARTICLE INFO

Article history:
Received 24 May 2018
Accepted 22 December 2018

Editor: Dr. S. Dancer

Keywords:
Polyamidoamine dendrimers
Skin
Biocide
Novel antiseptic
Antimicrobial

ABSTRACT

The aim of this study was to investigate a range of poly(amidoamine) (PAMAM) dendrimer generations against Gram-positive and Gram-negative skin pathogens and to determine any differences in antimicrobial potency for different generations, characterising how differences in physicochemical properties influence antimicrobial efficacy. A range of tests were carried out, including viable count assays to determine half maximal inhibitory concentration (IC_{50}) values for each dendrimer, membrane integrity studies and an inner membrane permeabilisation assay. This is supported by scanning electron microscopy imaging of the interactions observed between dendrimers and bacteria. The results of this study indicate that the antimicrobial efficacy of native PAMAM dendrimers is dependent on generation, concentration and terminal functionalities, for example, the concentration at 50% growth inhibition (MIC_{50}) (μg/mL), against *Staphylococcus* aureus was between 26.77 for the G2-PAMAM-NH_2 dendrimer and 2.881 for the G5-PAMAM-NH_2 dendrimer. There was a strong correlation between membrane disruption and the determined biocidal activity, making it a key contributing mechanism of action. This study demonstrates that selection of the type of PAMAM dendrimer is important as their inherent antimicrobial efficacy varies according to their individual physicochemical properties. This understanding may pave the way for the development of enhanced dendrimer-based antimicrobial formulations and drug-delivery systems.

1. Introduction

The skin is normally colonised by a diverse range of commensal microorganisms; when a patient's immune system is compromised or the skin barrier is impaired these microorganisms may then elicit an infection. Many such infections arise from the patient's own microbial flora, with the most prominent pathogen being *Staphylococcus aureus. S. aureus* typically resides within the anterior nares and perineum [1] and those patients colonised on hospital admission are at greater risk of developing surgical-site incision infections. It has also been shown to spread epidemically between patients and can be transferred from staff to patients, and vice versa [2].

Strategies in synthetic chemistry aimed at developing improved antimicrobials have traditionally focused on identifying orally bioavailable small drug molecules, often utilising high-throughput screening methods [3], an approach that has not yet translated into the availability of novel antibiotics in the clinic, particularly in light of growing microbial resistance. Biological targets, such as bacterial cell membranes, consist of macromolecules that rely on polyvalent interactions in their binding [4]. Most biological targets are of a nano-scale (1–100 nm) and therefore polyvalent macromolecules of a similar size may have increased biological efficacy when compared with small-molecule drugs due to a match in scale and multivalent binding [3]. For example, silver nanoparticles with a 1- to 10-nm size range were shown to have a greater direct interaction with bacteria than particles >10 nm in diameter [5], and silver complexes of polyamidoamine (PAMAM) dendrimers have been shown to be effective against S. *aureus, Escherichia coli* and *Pseudomonas aeruginosa* in vitro [6].

PAMAM dendrimers have become the most widely investigated dendrimers for a range of biomedical applications [7–9]. Their highly branched and globular nature gives them unique properties which enable them to function as a multivalent biocide or a nano-scale platform for antimicrobial drug delivery [10]. The uniform branching of dendrimers provides a large surface-area-to-volume ratio, enabling high reactivity with microorganisms in vivo [11]. The highly localized and dense occurrence of functional groups on the dendrimer's surface can be tailored for antimicrobial

‡ Corresponding author. Tel.: +44 1782 734 776.
E-mail address: g.p.j.moss@keele.ac.uk (G.P. Moss).
* Present address: School of Pharmacy and Medical Sciences, University of South Australia, Adelaide, South Australia, 5000.
† Present address: School of Pharmacy and Biomedical Sciences, University of Central Lancashire, Preston, UK.

https://doi.org/10.1016/j.ijantimicag.2018.12.012
0924-8579/

efficacy or for the conjugation of targeting ligands to a variety of a microorganism's receptors [12,13].

The antimicrobial properties of unmodified PAMAM dendrimers against ocular pathogens was explored by Calbaretta and co-workers [14]. They found that the amine terminated G5-PAMAM dendrimer was toxic to *P. aeruginosa* with the concentration at 50% growth inhibition (MIC_{50}) of 1.5 ± 0.1 μg/mL, but less so for *S. aureus* (20.8 ± 3.4 μg/mL). It was demonstrated that a partial coating of the amine groups with polyethylene glycol (PEG) reduced the toxicity of the G5-PAMAM against human corneal epithelial cells whilst retaining high toxicity against *P. aeruginosa* with a MIC_{50} of 0.9 ± 0.1 μg/mL. PEGylation of the G5-PAMAM resulted in a further decrease in efficacy against the Gram-positive *S. aureus* [14]. Further, they separately reported that, even though G5-PAMAM-NH_2 has a greater localisation of amines at its surface compared to G3-PAMAM, the potency was not increased [15].

Thus, the aim of this study was to investigate a range of PAMAM dendrimer generations, including amine- and carboxyl-terminated dendrimers, against Gram-positive and Gram-negative skin pathogens and to determine any differences in antimicrobial potency for different generations, and thus characterize how differences in molecular weights and surface charge affects antimicrobial efficacy.

2. Materials and Methods

2.1. Microdilution broth with viable count assay to determine inhibitory concentration (MIC_{50})

Bacterial culture-grade Petri dishes, universals and pipette tips were all purchased from Startstedt (Leicester, UK). Bacterial growth medium, Mueller–Hinton agar (MHA) and Mueller–Hinton broth (MHB) were obtained from Oxoid (Basingstoke, UK). The cation content (Mg^{2+} and Ca^{2+}) was adjusted in line with recommendations from the Clinical and Laboratory Standards Institute (CLSI) [16]. All salts used in diluents or media were reagent grade and purchased from Fisher (Loughborough, UK). *S. aureus* (ATCC 11832) and *E. coli* (ATCC 8277) were plated out on respective cation-adjusted MHA using a streak plate method to ensure growth of single colonies. The inoculated MHA plates were inverted and incubated at 37 ± 1°C for 18–24 h in aerobic conditions. After incubation, three to four single colonies were swabbed with a sterile loop and used to inoculate 10 mL of cation-adjusted MHB which was then incubated at 37 ± 1°C for 18 h. The dense overnight inoculum was then diluted to an absorbance of 0.140 using an ultraviolet–visible spectroscopy (UV-Vis) spectrophotometer (Hitachi, U1-900, Berkshire, UK) to achieve an inoculum density of ~10^7 cells/mL. The bacterial cell density at an absorbance of 0.140 was confirmed by diluting the bacteria and counting the cells using a haemocytometer. The inoculum was then further diluted in cation adjusted MHB to achieve a test inoculum of 1×10^5 cells/mL.

PAMAM dendrimers (generations G2–G5; Sigma Aldrich, Dorset, UK) at varying concentrations in methanol (MeOH) were prepared at concentrations ranging from 500 to 1 μg/mL in ultrapure sterile water. Each PAMAM dendrimer concentration was tested in triplicate and 50 μL of each solution was plated on to a sterile 96-well plate. Fifty microlitres of the inoculum was added to each well, except for three wells with cation-adjusted MHB and sterile water only as a sterility control. A growth control was tested in parallel without the addition of PAMAM dendrimer and a positive control of gentamicin 1 mg/mL was included. The 96-well plate was then incubated at 37 ± 1°C for 2 h and shaken at 200 rpm.

After a 2-h incubation period, each well (excluding sterility control) was serially diluted 1:10 in cation-adjusted MHB to achieve a range of dilutions down to 1:100,000 and then further agitated using a sterile pipette tip. Fifty microlitres of each dilution was plated onto a Petri dish using the pour plate method with the addition of 25 mL of molten MHA at 45°C. The plates were then inverted and incubated for 18–24 h at 37 ± 1°C in aerobic conditions. Post-incubation, bacterial colonies on each plate were manually counted using a click counter. The dilutions where 30–300 colony forming units (CFUs) had grown for each growth control or PAMAM test concentration were selected. Each test concentration was tested in triplicate and the inhibition percentage was calculated using the following equation:

$$Inhibition\ percentage\ \% = \left(100 - \left(\frac{treated\ count}{growth\ control\ count}\right) \times 100\right) \quad (1)$$

The data was then plotted as a graph of log (inhibitor) versus normalized response to determine the MIC_{50} (Eqn. 2) usingGraphPad Prism®version 5 (San Diego, USA).

$$Y = \frac{100}{\left(1 + 10^{((LogIC50 - X) \times Hillslope)}\right)} \quad (2)$$

The log (dose) response curve follows a sigmoidal curve and the data was normalized to the growth control as 100%. The normalized model forces the curve from 0% to 100%. This is ideal for the calculation of the MIC_{50}. This model also does not assume a standard hill slope of 1.0 but fits the hill slope from the data therefore it is a variable slope model that is ideal when there are many data points. The broth microdilution assays to calculate the MIC_{50} concentrations were run as n=9, therefore this model was ideal.

2.2. Membrane integrity study

The membrane integrity study was modified from the method outlined in Chen and Cooper [27]. *S. aureus* (ATCC 11832), *Staphylococcus epidermidis* (ATCC 12228) and *E. coli* (ATCC 8277) were plated on tryptone soya agar (TSA) plates using a streak method. The inoculated plates were inverted and incubated at 37 ± 1°C for 18–24 h in aerobic conditions. After the incubation period, two to three single colonies were removed using a sterile loop and used to inoculate tryptone soya broth (TSB). The inoculated TSB was then incubated for 18 h at 37 ± 1°C. Post-incubation period the inoculated TSB was then centrifuged at 1000 × *g* for 10 min to harvest the bacterial cells, with the resultant pellet resuspended in 1 × phosphate-buffered saline (PBS, pH 7.4). This was centrifuged (as above) and the supernatant discarded. The pellet was washed and resuspended in PBS and the absorbance was adjusted to 0.7 at 420 nm to dilute the cells to a final test suspension. A 3-mL aliquot of the final bacterial inoculum was added to a 3-mL aliquot of the PAMAM dendrimer solution at a concentration of 10 × the calculated MIC_{50} for each respective PAMAM dendrimer generation. At different time points (20, 40, 60 and 120 min) a 1.5-mL aliquot of the sample was removed and immediately syringe-filtered using a 0.22-μm syringe filter (Millipore MCE sterile 33-mm filter, Watford, UK). The particulate-free supernatant was analysed at 260 nm by UV spectrometry (Hitachi, U1-900, Berkshire, UK), with the absorbance being plotted against each time point.

2.3. Inner membrane permeabilisation assay

Inner membrane permeabilisation was determined by the release of cytoplasmic β-galactosidase from *E. coli* into the culture medium in a method modified from Je and Kim [28]. *E. coli* was cultured, harvested and washed and re-suspended in 0.5% NaCl. *E. coli* was re-suspended at an absorbance of 0.6 at 420 nm and 100 μL of the test inoculum was transferred into each well of a 96-well plate. One-hundred microlitres of PAMAM dendrimer (generations 2, 3, 3.5, 4 and 5 at concentrations of 0.1, 1, 5, 10, 25 and

Table 1
Dendrimer physicochemical characteristics and calculated the concentration at 50% growth inhibition (MIC_{50}) (μg/mL) with 95% confidence intervals against *Staphylococcus aureus* and *Escherichia coli*.

Bacteria	PAMAM generation	Molecular weight (g/mol)	No. of amine surface groups	MIC_{50} (95% CI) μg/mL
S. aureus	G2-PAMAM-NH_2	3256	16	26.77 (22.58–31.75)
	G3-PAMAM-NH_2	6909	32	9.374 (7.88–11.15)
	G4-PAMAM-NH_2	14,215	64	5.962 (5.375–6.614)
	G5-PAMAM-NH_2	28,826	128	2.881 (2.473–3.355)
	G3.5-PAMAM-COOH	12,927	64	>250
E. coli	G3-PAMAM-NH_2	6,909	32	4.931 (4.28–5.679)
	G3.5-PAMAM-COOH	12,927	64	>1000

CI, confidence interval.

50 μg/mL) was added to each well. Also, 10 μL of a 30-mM *ortho*-nitrophenyl-β-galactoside (ONPG; Sigma, Dorset, UK) solution was added to each well. A blank of *E. coli* with ONPG without PAMAM dendrimer was used as a negative control and a vehicle control was also run in parallel. The production of *O*-nitrophenol was measured every 2 min for 12 min by monitoring the absorbance at 420 nm in a microplate reader (Biotek, Northstar, Bedfordshire, UK).

2.4. Scanning electron microscopy of bacteria challenged with PAMAM dendrimers

S. aureus (ATCC 11832) and *E. coli* (ATCC 8277) were cultured, harvested and washed as described above except that an overnight culture of 10^8 cells/mL was used to ensure that bacterial cells were at a sufficiently high density after the washes involved in preparation methods. Two-hundred-microlitre aliquots of a range of concentrations of each dendrimer (from 1 to 200 μg/mL for G2, G3 and G4-PAMAM-NH_2, and 0.0025–12.5 μg/mL for G5-PAMAM-NH_2) were constituted. For G3.5-PAMAM-COOH dendrimer the concentration range of solutions made were between 1 and 250 μg/mL. The PAMAM dendrimer solutions (200 μL) were added to 200 μL of the bacterial inoculum and incubated at 37 ± 1°C for 2 h and shaken at 200 rpm. After the incubation period the bacteria were centrifuged at 10,000 × *g* for 10 min, resuspended in PBS (pH 7.4), centrifuged as above and the supernatant discarded. This was repeated three times to wash the harvested bacteria. The bacteria were then fixed in 2.5% glutaraldehyde in 0.1 M sodium cacodylate buffer (pH 7.4 containing 2 mM $CaCl_2$) for 2 h on a low-speed rotator.

Fixative was washed from the bacteria in sodium cacodylate buffer (pH 7.4 containing 2 mM $CaCl_2$) three times. A 100-μL aliquot of each fixed sample was added to a poly-*L*-lysine-coated coverslip. The bacteria on the poly-*L*-lysine coated coverslips were then post-fixed in a solution of 1% sodium tetroxide in sodium cacodylate buffer. After a 1-h contact time the osmium tetroxide was removed by washing the coverslips in sodium cacodylate buffer (pH 7.4 containing 2 mM $CaCl_2$). The coverslips were then submerged in 70% ethanol and dehydrated at 4°C for 6 days. The samples were then further dehydrated for 10 min each in 70%, 80%, 90% and 100% ethanol. To remove the solvent from the samples they were critical-point dried three times to replace the 100% ethanol with liquid CO_2 under pressure. Liquid CO_2 was subsequently removed by increasing the temperature (to 40°C) and pressure until the CO_2 vaporised. Samples were secured to a scanning electron microscope (SEM) stub mount, sputtered with gold and then placed in the high-resolution (1.5 nm) field emission SEM (Hitachi, S4500).

2.5. Statistical analysis of results

Results are reported as the mean ± standard error of the mean unless otherwise stated. All inner membrane permeabilisation data passed the D'Agostino and Pearson normality test ($\alpha = 0.05$) using GraphPad Prism® version 5 (San Diego, USA). For the inner membrane permeabilisation data a two-way ANOVA with a Bonferroni post-test was used to compare the two variables of dendrimer generation and dendrimer concentration at the various time points.

3. Results

3.1. Microdilution broth with viable count assay to determine the inhibitory concentration (MIC_{50})

The inhibitory effect of PAMAM dendrimers against *S. aureus* and *E. coli* is shown in Table 1. For 50% inhibition of *S. aureus* the G2-PAMAM-NH_2 dendrimer required greater than nine-times the concentration that was required for the G5-PAMAM-NH_2 dendrimer to exert the same effect. An increase in PAMAM generation from G2 to G5 showed that the MIC_{50} (*S. aureus*) decreased substantially (Table 1). For the lowest concentrations of G2-PAMAM-NH_2 and G5-PAMAM-NH_2 tested, bacterial growth was observed when compared to the untreated growth control. The MIC_{50} required to inhibit 50% of the *S. aureus* was approximately two-fold higher than the concentration required to inhibit 50% of the *E. coli*. When challenged with *S. aureus* the carboxyl-terminated dendrimer resulted in minimal inhibition (Table 1). The MIC_{50} against *S. aureus* decreased with increasing numbers of surface amine groups on the PAMAM dendrimer (Fig. 1). An exponential inhibition curve was added to the graph which highlights the exponential increase in molecular weight and the number of amine surface groups with increasing PAMAM generation.

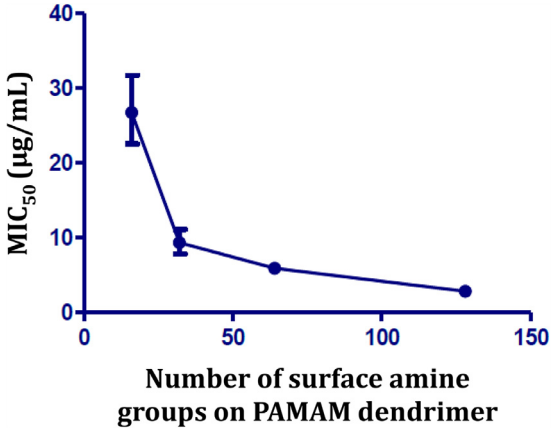

Fig. 1. Calculated concentration at 50% growth inhibition (MIC_{50}) (μg/mL) concentrations. MIC_{50} (μg/mL) with error bars representing 95% confidence intervals (n=3) against *Staphylococcus aureus* plotted against the theoretical number of surface amine groups corresponding to G2-PAMAM-NH_2, G3-PAMAM-NH_2, G4-PAMAM-NH_2 and G5-PAMAM-NH_2 dendrimers.

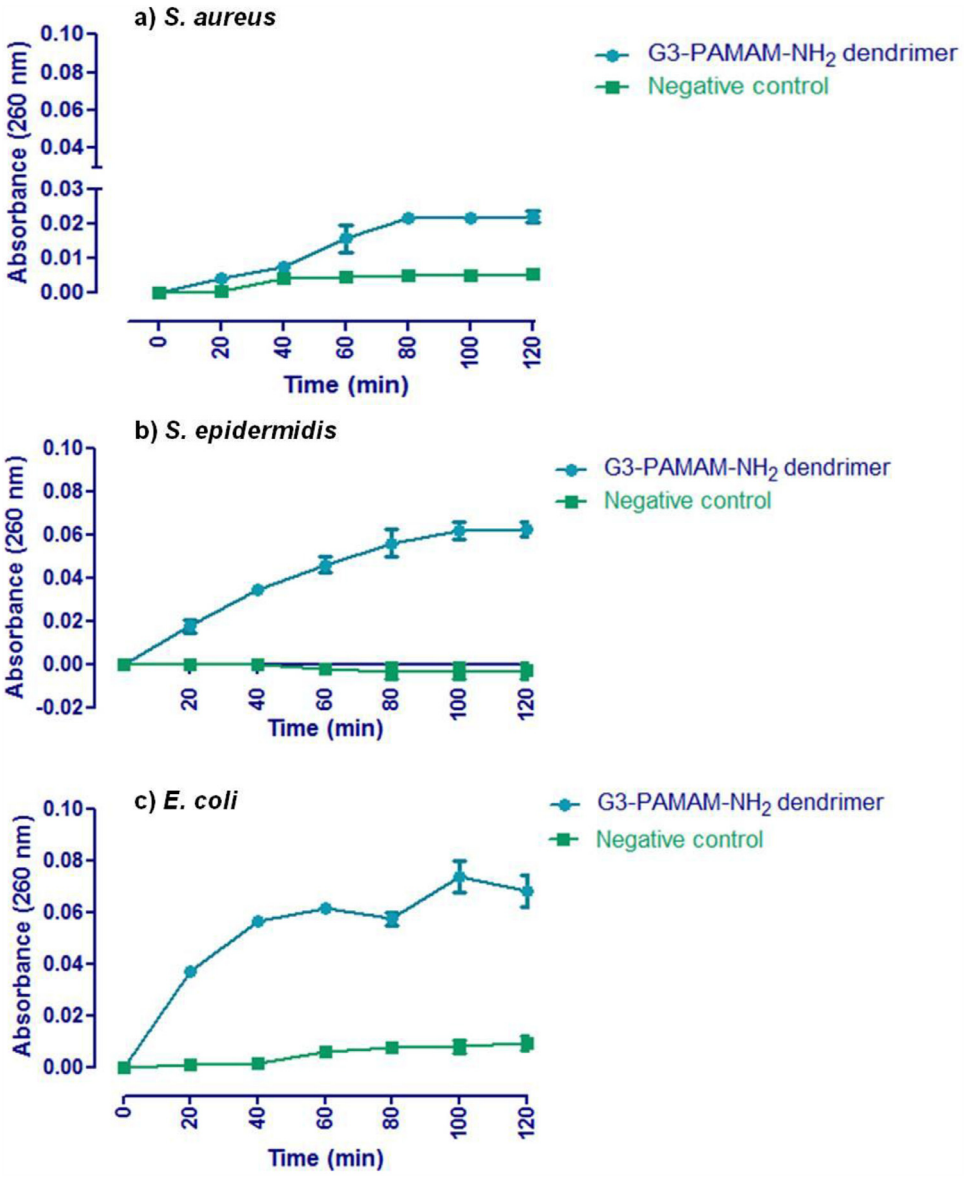

Fig. 2. The release of nuclear material from *Staphylococcus aureus, Staphylococcus epidermidis* and *Escherichia coli.* (A) Absorbance at 260 nm plotted against time for *S. aureus* challenged against G=3 × 5 MIC_{50}; (B) absorbance at 260 nm plotted against time for *S. epidermidis* challenged against G=3 × 5 MIC_{50}; (C) absorbance at 260 nm plotted against time for *E. coli* challenged against G=3 × 5 MIC_{50}. MIC_{50} is the concentration at 50% growth inhibition. All results are displayed as (n=3) mean ± standard deviation. Negative control was the absorbance at 260 nm for the untreated bacteria group.

3.2. Membrane integrity study

Fig. 2 indicates that, for all three bacterial strains, the absorbance at 260 nm increased with time with a plateau at 80 min (for *S. aureus*) and 100 min for both *S. epidermidis* and *E. coli*, respectively. The absorbance increase for *S. aureus* shows a linear trend to a plateau with data overlapping with the control up to 40 min, whereas with the absorbance for *S. epidermidis* increased monotonically up to a plateau at 100 min. *E. coli* showed an increase in absorbance over the first 60 min.

3.3. Inner membrane permeabilisation assay

In the inner membrane permeabilisation assay it was found that the absorbance reached a plateau at around 20 min. The mean absorbance at 420 nm for G2-PAMAM-NH_2, G3-PAMAM-NH_2, G4-PAMAM-NH_2, and G5-PAMAM-NH_2 was 0.222 (95% confidence interval (CI): 0.221–0.224) 0.228 (95% CI: 0.227–0.230), 0.228 (95% CI: 0.226–0.229) and 0.214 (95% CI: 0.213–0.216), respectively. A clear effect of concentration dependency on the inner membrane permeabilisation was observed when the vehicle control was compared to 5 μg/mL,when the concentrations 0.1 and 1.0 μg/mL of dendrimers were compared, there was no statistical difference (P>0.05). The inner membrane permeabilisation and thus production of *O*-nitrophenol, increased with increasing concentrations of the PAMAM dendrimer and with time (Fig. 3). For all four PAMAM-NH_2 dendrimer generations tested, a concentration as low as 5 μg/mL resulted in permeabilisation of the inner membrane by 12 min (Fig. 3). The production of *O*-nitrophenol varied across the four PAMAM generations tested. The highest concentration tested (50 μg/mL) demonstrated the greatest increase in absorbance, therefore inducing the highest degree of inner membrane permeabilisation. However, the exception to this was the G5-PAMAM-NH_2 dendrimer. At a particular time point of 4–10 min, 25 μg/mL solution of G5-PAMAM-NH_2 dendrimer showed a higher absorbance at 420 nm and thus *O*-nitrophenol production than at a

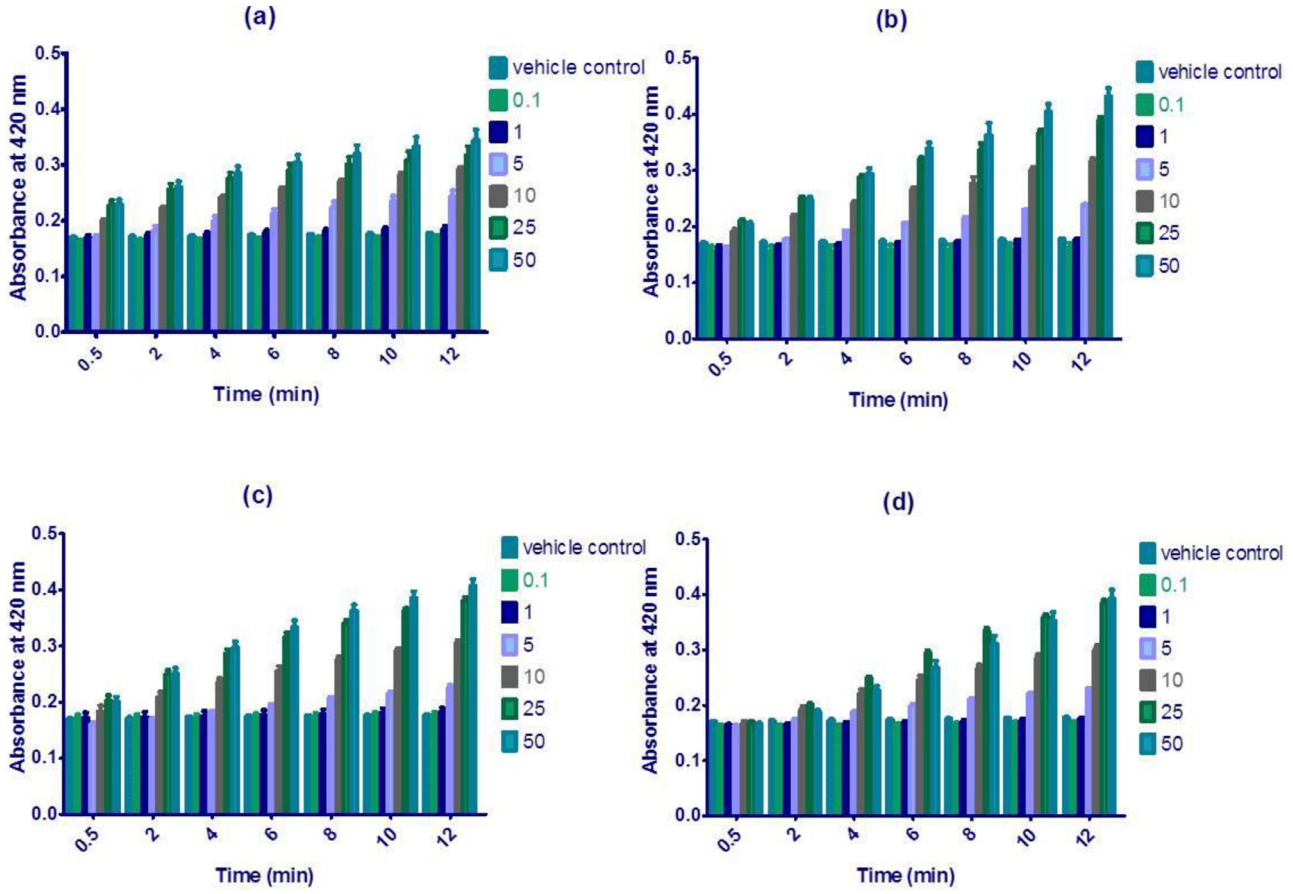

Fig. 3. The relationship between concentration, time and dendrimer generation on the inner membrane permeabilisation of *Escherichia coli*. (A) G2-PAMAM-NH_2-treated *E. coli*; (B) G3-PAMAM-NH_2-treated *E. coli*; (C) G4-PAMAM-NH_2-treated *E. coli*; and (D) G5- PAMAM-NH_2-treated *E. coli*. Vehicle control is displayed as the untreated control group. All results shown represent the mean ± standard error of the mean (n=3)

50 μg/mL concentration. G5-PAMAM-NH_2 dendrimer also demonstrated a longer lag period for absorbance increase at 420 nm due to its high molecular weight and diameter causing slow passive diffusion across the cell wall and membrane. At a concentration of 5 μg/mL and based on the mean across all time points for a specific concentration, the order from the highest absorbance and thus production of o-nitrophenol to the lowest was G2>G3>G5>G4. At a higher dendrimer concentration of 50 μg/mL the absorbance measurement trend in decreasing order was G3>G4>G2>G5.

A final measurement of *O*-nitrophenol production was taken at 60 min (Fig. 4). It was established that even after 60 min no change in absorbance was observed for concentrations below 5 μg/mL (P>0.05). With the exception of 0.1 and 1 μg/mL of PAMAM dendrimer, there was a significant difference in absorbance when comparing all concentrations of each PAMAM generation to the vehicle control (P<0.001). A generation effect was also observed, to a degree, when comparing the absorbance at 420 nm of various PAMAM dendrimer generations over 12 min at 50 μg/mL (Fig. 5).

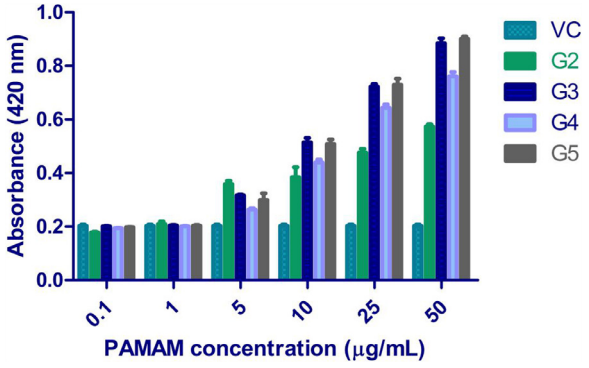

Fig. 4. The inner membrane permeabilisation of *Escherichia* coli at 60 min for a range of dendrimer concentrations. Absorbance at 420 nm plotted against a range of dendrimer concentrations (0.1–50 μg/mL) at 60 min. G2 corresponds to G2-PAMAM-NH_2-treated *E. coli*, G3 to G3-PAMAM-NH_2-treated *E. coli*, G4 to G4-PAMAM-NH_2-treated *E. coli* and G5 to G5-PAMAM-NH_2-treated *E. coli*. VC corresponds to the vehicle control and is displayed as the untreated bacteria group control. All results shown represent the mean ± standard error of the mean (n=3). All PAMAM-treated samples are significantly different (P<0.001) from the vehicle control for the concentration range 5–50 μg/mL.

3.4. Scanning electron microscopy of bacteria challenged with PAMAM dendrimers

Fig. 6 (A,B) shows an electron micrograph of *S. aureus* bacteria. When compared to the G3-PAMAM-NH2 at a concentration of five-times the MIC_{50} (μg/mL), varying degrees of membrane damage was observed from minor blebbing through to total destruction of the cell membrane and cell wall (Fig. 6 C,D). This was also found to be the case with G2-PAMAM-NH2 (Fig. 6 E,F) and G5-PAMAM-NH2 (Fig. 6 G,H). The SEM images demonstrate the ability for G2-PAMAM-NH2 and G5-PAMAM-NH2 to cause severe bacterial cell membrane and cell wall damage, including blebbing of cytoplasmic contents from damaged cell, and in some cases complete cell lysis. Sheets of bacterial cell wall and cytoplasmic content debris can be observed in the PAMAM treated bacteria images

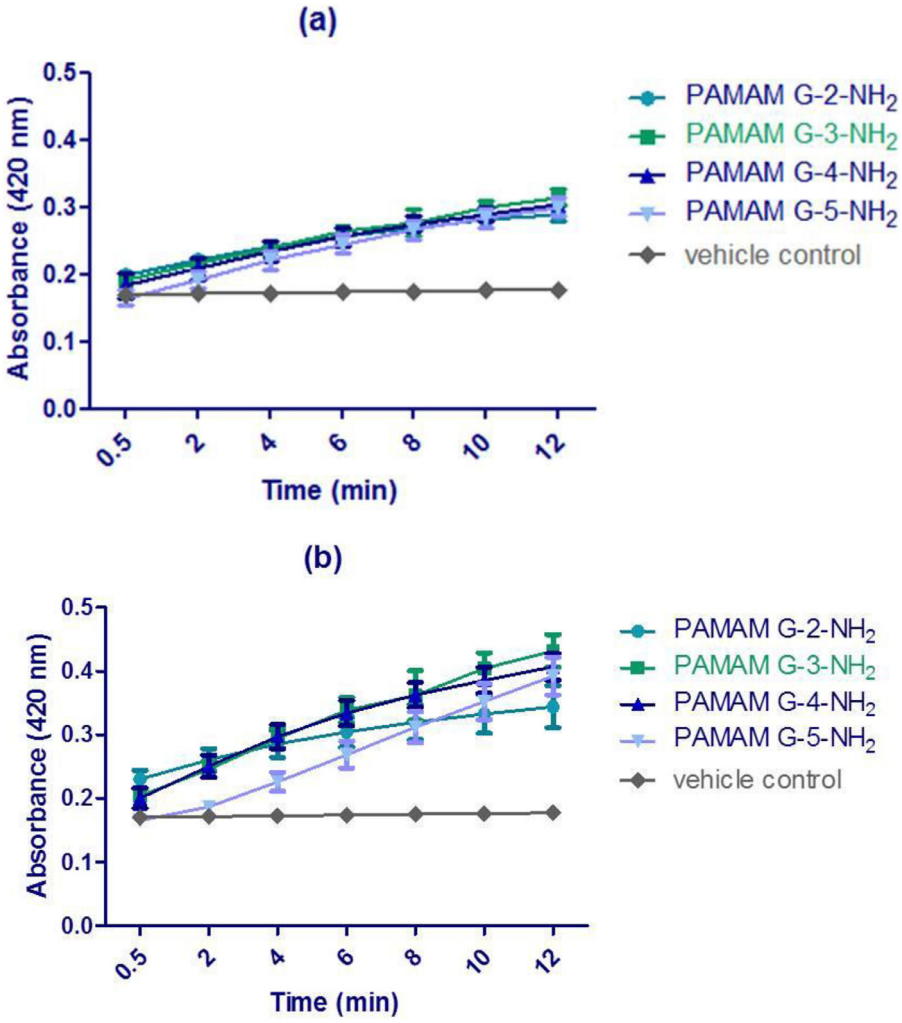

Fig. 5. The effect of dendrimer generation and time at specific concentrations on the inner membrane permeabilisation of *Escherichia coli.* Absorbance at 420 nm plotted against time in minutes, (A) corresponds to each PAMAM generation at a concentration of 10 μg/mL challenged against *E. coli* and (B) PAMAM generations at a concentration of 50 μg/mL challenged against *E. coli.* VC corresponds to the vehicle control and was displayed as the untreated bacteria group control. All results shown represent the mean ± standard error of the mean (n=3). All treated sample values are significantly different (P<0.05) from the vehicle control with the exception of the 0.5-min time points and 2 min for G5-PAMAM at both concentrations tested.

(Fig. 6 A–H). For G3.5-PAMAM-COOH at a concentration of 1 mg/mL (Fig. 6 I,J) there was no difference in bacterial cell morphology or changes to the integrity of the bacterial cell membrane or cell wall when compared to the untreated *S. aureus* group.

SEM images were also collected for the Gram-negative, rod-shaped *E. coli* bacteria. Fig. 7 (A,B) shows the intact PAMAM untreated group micrographs. Fig. 7 (C,D) illustrates the G3-PAMAM-NH_2-treated group. Damage to the bacterial wall and cell membranes can be observed due to leakage of the cytoplasmic contents from the cell and blebbing. The PAMAM dendrimer typically targeted the polar regions of the *E. coli* rods, consistent with the findings observed by others [25]. Again, no changes in cell morphology were observed for the G3.5-PAMAM-COOH at a concentration of 1 mg/mL.

4. Discussion

A clear, generation-dependent trend was observed when the MIC_{50} of each PAMAM generation was related to their respective theoretical number of surface amine groups. There was an inverse correlation between the MIC_{50} concentration and PAMAM dendrimer generation. It was found that by increasing the number of amine groups on the dendrimer surface the concentration required to inhibit 50% of the bacteria dramatically decreased. Enhanced destabilisation of bacterial membranes has been observed by increasing the number of amino groups on a polycation [17]. This generation-dependent trend was contrary to the findings elsewhere [15] where it was observed that the MIC for G3-PAMAM-NH_2 and G5-PAMAM-NH_2 against *S. aureus* was identical. A distinction in MIC value was found for two different PAMAM generations against *P. aeruginosa* as G3-PAMAM-NH_2 and G5-PAMAM-NH_2 exhibited a MIC of 6.3 μg/mL and 12.5 μg/mL, respectively. The authors suggest the difference is due to the G3-PAMAM-NH_2 dendrimer's ability to penetrate the cell more easily due to its lower molecular weight compared to G5-PAMAM-NH_2. This effect was not observed in the present study, possibly due to differences in the chemical nature of the G3 and G5 dendrimers used in our study and the study by Lopez et al., respectively [15].

Another apparent trend is that PAMAM dendrimers are more effective against Gram-negative bacteria such as *E. coli*., a finding echoed elsewhere [14]. *E. coli* has a very different cell wall structure and composition compared to the Gram-positive *S. aureus*. The outer membrane of *E. coli.* consists of lipopolysaccharide (LPS), phospholipids and proteins [18]. LPS carries a high anionic charge at physiological pH due to the ionisable phosphoryl and carboxyl groups [19]. The polycationic nature of PAMAM dendrimers

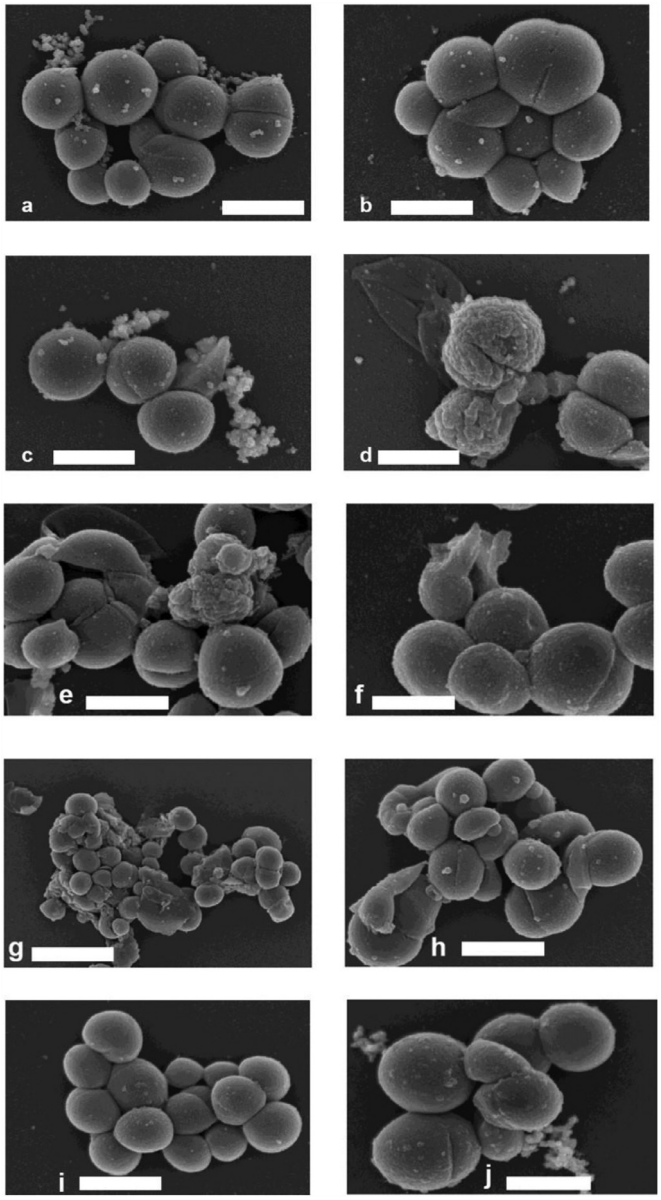

Fig. 6. Scanning electron micrographs of *Staphylococcus aureus* challenged with PAMAM dendrimer. (A) Untreated *S. aureus* at a magnification of × 25k, scale bar represents 1 µm. (B) untreated *S. aureus* at a magnification of × 30k, scale bar represents 1 µm. (C) *S. aureus* treated with G3-PAMAM-NH_2 at a concentration of 5 × calculated half maximal inhibitory concentration (IC_{50}). Magnification × 30k and scale bar represents 1 µm. (D) S. aureus treated with G3-PAMAM-NH_2 at a concentration of 5 × calculated IC_{50}. Magnification × 30k and scale bar represents 1 µm. (E) *S. aureus* treated with G2-PAMAM-NH_2 at a concentration of 250 µg/mL, magnification × 25k and scale bar represents 1 µm. (F) *S. aureus* treated with G2-PAMAM-NH_2 at a concentration of 250 µg/mL, magnification × 40k and scale bar represents 1 µm. (G) *S. aureus* treated with G5-PAMAM-NH_2 at a concentration of 250 µg/mL, magnification × 10k and scale bar represents 3 µm. (H) *S. aureus* treated with G5-PAMAM-NH_2 at a concentration of 250 µg/mL, magnification × 20k and scale bar represents 1 µm. (I) *S. aureus* treated with G3.5-PAMAM-COOH at a concentration of 1000 µg/mL, magnification × 25k and scale bar represents 1 µm. (J) *S. aureus* treated with G3.5-PAMAM-COOH at a concentration of 1000 µg/mL, magnification × 30k and scale bar represents 1 µm.

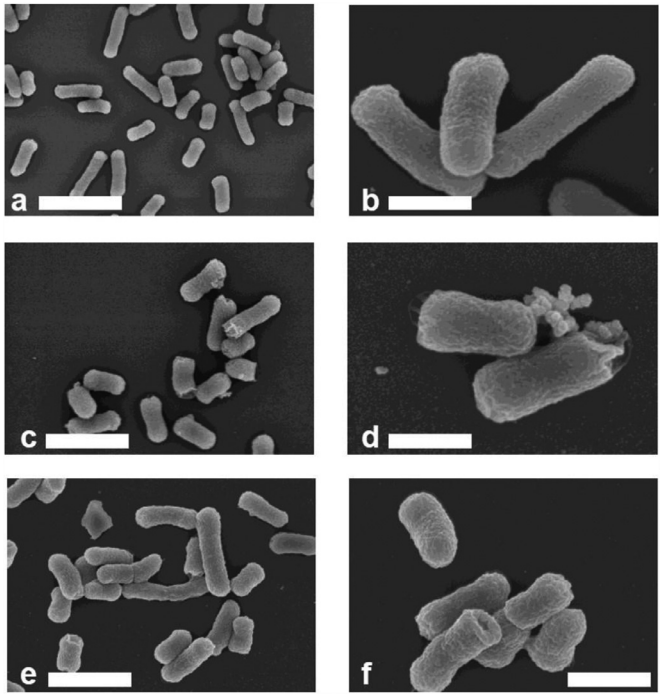

Fig. 7. Scanning electron micrographs of *Escherichia coli* challenged with PAMAM dendrimer. (A) *E. coli* untreated, magnification × 10k, scale bar represents 2 µm. (B) *E. coli* untreated, magnification × 40k, scale bar represents 1.5 µm. (C) *E. coli* treated with G3-PAMAM-NH_2 at a concentration of 5 × calculated half maximal inhibitory concentration (IC_{50}), magnification × 15k, and scale bar represents 2 µm. (D) *E. coli* treated with G3-PAMAM-NH_2 at a concentration of 5 × calculated IC_{50}, magnification × 50k, and scale bar represents 1.5 µm. (E) *E. coli* treated with 1000 µg/mL of G3.5-PAMAM-COOH, magnification × 15k scale bar represents 2 µm. (F) *E. coli* treated with 1000 µg/mL of G3.5-PAMAM-COOH, magnification × 30k, scale bar represents 1.5 µm.

ensures high reactivity with, and affinity for, the outer membrane due to strong electrostatic forces. The high degree of interaction and disruption of the lipid bilayer of the outer membrane with the polycationic PAMAM dendrimer, reported previously [14], is one possible explanation for the enhanced antimicrobial efficacy observed for Gram-negative bacteria and for G5-PAMAM-NH_2 tested against *P. aeruginosa*.

The results indicate that G3- PAMAM-NH_2 causes intracellular components to leak from *S. aureus, S. epidermidis* and *E. coli* within approximately 20 min. Precipitation and coagulation of nucleotides has been observed for other cations [20] and has potentially occurred with the concentration of PAMAM dendrimer. The inner membrane consists of a complex proteome within a lipid bilayer. This is formed principally from phosphatidyl ethanolamine, phosphatidyl glycerol, and to a lesser extent cardiolipin, the latter two of which carry anionic charges [21]. Our results indicate that the polycationic PAMAM dendrimers have a strong affinity for the anionic inner membrane of *E. coli*. These novel results suggest that there are important time-, concentration- and dendrimer-generation-dependent effects on the inner membrane permeabilisation of *E. coli*.

Structural and morphological changes induced by the dendrimers are shown in Figs. 6 and 7. The *S. aureus* samples showed blebbing of cytoplasmic material on the cell surface that had been presumably extruded from a damaged cell membrane. Leaked cytoplasmic material, severe membrane damage and even separation of the cell membrane of the bacteria from the cell was also observed, caused by the different generations of PAMAM dendrimers. The degree of cell damage observed is consistent with previous studies of the cationic biocides polyquaternium-1 and myristamidopropyl dimethylamine [22]. Further, comparable cytoplasmic membrane damage was observed for *S. aureus* when challenged with the essential oil isolated from *O. Vulgare* [23]. Marked release of cytoplasmic contents was also observed for *E. coli* due to membrane damage inflicted by the G3-PAMAM-NH_2 dendrimer, which is again

consistent with previous findings with tea tree oil [24] and, in one case, with the G4-PAMAM-NH_2 dendrimer [25], which resulted in rupturing of cell walls, erosion of cell membranes and shrinkage of bacterial cells. Thus, the SEM images herein suggest that the mechanism of action of PAMAM dendrimers is to target and disrupt the bacterial cell membrane.

5. Conclusions

This study has confirmed that the antimicrobial efficacy of native PAMAM dendrimers is dependent on generation, concentration and terminal functionalities. There was a strong correlation between membrane disruption and the determined biocidal activity, thus making it a key contributor to the mechanism of action. This study has shown that selection of the type of PAMAM dendrimer is important as their inherent antimicrobial efficacy is dependent on the physicochemical properties of specific dendrimers. Such correlations between structure and biocide function will allow a more appropriate and focused use of dendrimers in this role. Recently, for example, it was reported that following the pre-treatment of skin with a G3-PAMAM dendrimer, the subsequent skin permeation of chlorhexidine was significantly enhanced. This clearly indicates that the strategy for increasing antimicrobial efficacy with dendrimers is viable, either as a single treatment or in combination with other treatments [26]. G5-PAMAM-NH_2 dendrimer would also be the most suitable polymer for biocidal applications as it shows the greatest efficacy against both Gram-negative and Gram-positive bacteria. Thus, this study clearly demonstrates the antimicrobial potential of dendrimers and that optimising their efficacy is based on dendrimer physicochemical properties. Through this understanding an informed choice may be made as to which PAMAM dendrimer to select as part of a quality-by-design approach to developing novel biocides.

Acknowledgements

The authors would like to acknowledge and thank Professor Stephen Chapman (School of Pharmacy, Keele University, UK) for his assistance with this study.

Funding

This work was funded by an Engineering and Physical Sciences Research Council (EPSRC) CASE award (R4504 A779) in collaboration with Dermal Technology Laboratory Ltd.

Competing Interests

The authors have no conflicts of interest to disclose.

Ethical Approval

Not required.

References

[1] Davis KA, Stewart JJ, Crouch HK, Florez CE, Hospenthal DR. Methicillin-resistant Staphylococcus aureus (MRSA) nares colonization at hospital admission and its effect on subsequent MRSA infection. Clin Infect Disease 2004;39:776–82.
[2] Von Eiff C, Becker K, Machka K, Stammer H, Peters G. Nasal carriage as a source of Staphylococcus aureus bacteremia. New Eng J Med 2001;344:11–16.
[3] McCarthy TD, Karellas P, Henderson SA, Giannis M, O'Keefe DF, Heery G, et al. Dendrimers as drugs: discovery and preclinical and clinical development of dendrimer-based microbicides for HIV and STI prevention. Mol Pharmacol 2005;2:312–18.
[4] Mammen M, Choi SK, Whitesides GM. Polyvalent interactions in biological systems: implications for design and use of multivalent ligands and inhibitors. Angewandte Chemie Int Edn 1998;37:2754–94.
[5] Morones JR, Elechiguerra JL, Camacho A, Holt K, Kouri JB, Ramirez JT, et al. The bactericidal effect of silver nanoparticles. Nanotech 2005;16:2346–53.
[6] Balogh L, Swanson DR, Tomalia DA, Hagnauer GL, McManus AT. Dendrimer-silver complexes and nanocomposites as antimicrobial agents. Nano Lett 2001;1:18–21.
[7] Svenson S. Dendrimers as versatile platform in drug delivery applications. Eur J Pharm Biopharm 2009;71:445–62.
[8] Esfand R, Tomalia DA. Poly (amidoamine)(PAMAM) dendrimers: from biomimicry to drug delivery and biomedical applications. Drug Discov Today 2001;6:427–36.
[9] Sajja HK, East MP, Mao H, Wang AY, Nie S, Yang L. Development of multifunctional nanoparticles for targeted drug delivery and non-invasive imaging of therapeutic effect. Curr Drug Discov Technol 2009;6:43–51.
[10] Meyers SR, Juhn FS, Griset AP, Luman NR Grinstaff MW. Anionic amphiphilic dendrimers as antibacterial agents. J Am Chem Soc 2008;130:1444–5.
[11] Zhang L, Pornpattananangkul D, Hu C, Huang C. Development of nanoparticles for antimicrobial drug delivery. Curr Med Chem 2010;17:585–94.
[12] Tomalia DA, Naylor AM, Goddard WA. Starburst dendrimers: molecular-level control of size, shape, surface chemistry, topology, and flexibility from atoms to macroscopic matter. Angewandte Chemie Int Edn 1990;29:138–75.
[13] Gillies ER, Frechet JMJ. Dendrimers and dendritic polymers in drug delivery. Drug Discov Today 2005;10:35–43.
[14] Calabretta MK, Kumar A, McDermott AM, Cai C. Antibacterial activities of poly (amidoamine) dendrimers terminated with amino and poly (ethylene glycol) groups. Biomacromolecules 2007;8:1807–11.
[15] Lopez AI, Reins RY, McDermott AM, Trautner BW, Cai C. Antibacterial activity and cytotoxicity of PEGylated poly (amidoamine) dendrimers. Mol Biosystems 2009;5:1148–56.
[16] Rennie R. NCCLS: Evaluation of Lots of Dehydrated Mueller-Hinton Broth for Antimicrobial Susceptibility Testing; Proposed Guideline, Wayne, Pennsylvania-aUSA: NCCLS; 2001. NCCLS document M32-P [ISBN 1-56238-447-3]940 West Valley Road, Suite 140019087-1898.
[17] Katsu T, Nakagawa H, Yasuda K. Interaction between polyamines and bacterial outer membranes as investigated with ion-selective electrodes. Antimicrob Agent Chemother 2002;46:1073–9.
[18] Nikaido H. Multidrug efflux pumps of gram-negative bacteria. J Bacteriol 1996;178:5853–9.
[19] Beveridge T.J. Structures of gram-negative cell walls and their derived membrane vesicles. J Bacteriol 999;181:4725-33.
[20] Hugo W, Longworth A. Effect of chlorhexidine diacetate on "protoplasts" and spheroplasts of *Escherichia coli*, protoplasts of *Bacillus megaterium* and the gram staining reaction of *Staphylococcus aureus*. J. Pharm Pharmacol 1964;16:751–8.
[21] Dowhan W. Molecular basis for membrane phospholipid diversity: why are there so many lipids? Ann Rev Biochem 1997;66:199–232.
[22] Codling CE, Hann AC, Maillard JY, Russell A. An investigation into the antimicrobial mechanisms of action of two contact lens biocides using electron microscopy. Cont Lens Anterior Eye 2005;24:163–8.
[23] De Souza EL, Barros JC, De Oliveira CEV, Da Conceicao ML. Influence of *Origanum vulgare* L. essential oil on enterotoxin production, membrane permeability and surface characteristics of *Staphylococcus aureus*. Int J Food Microbiol 2010;137:308–11.
[24] Gustafson J, Liew Y, Chew S, Markham J, Bell H, Wyllie S, et al. Effects of tea tree oil on *Escherichia coli*. Lett Appl Microbiol 1998;26:194–8.
[25] Wang B, Navath RS, Menjoge AR, Balakrishnan B, Bellair R, Dai H, et al. Inhibition of bacterial growth and intramniotic infection in a guinea pig model of chorioamnionitis using PAMAM dendrimers. Int J Pharm 2010;395:298–308.
[26] Holmes AM, Scurr DJ, Heylings JR, Wan KW, Moss GP. Dendrimer pre-treatment enhances the skin permeation of chlorhexidine digluconate: Characterisation by in vitro percutaneous absorption studies and Time-of-Flight Secondary Ion Mass Spectrometry. Eur J Pharm Sci 2017;104:90–101.
[27] Chen CZ, Cooper SL. Interactions between dendrimer biocides and bacterial membranes. Biomat 2002;23:3359–68.
[28] Je JY, Kim SK. Chitosan derivatives killed bacteria by disrupting the outer and inner membrane. J Agric Food Chem 2006;54:6629–33.